Desalination and Water Treatment
www.deswater.com
doi:10.5004/dwt.2017.20303

76 (2017) 19–29
May

Performance analysis of cascaded membrane distillation arrangements for desalination of brackish water

A. Najib[a], J. Orfi[a], E. Ali[b,*], A. Ajbar[b], M. Boumaaza[b], K. Alhumaizi[b]

[a]*Mechanical Engineering Department, King Saud University, Riyadh, Saudi Arabia, email: anmohammed@ksu.edu.sa (A. Najib), orfij@ksu.edu.sa (J. Orfi)*
[b]*Chemical Engineering Department, King Saud University, Riyadh, Saudi Arabia, email: amkamal@ksu.edu.sa (E. Ali), aajbar@ksu.edu.sa (A. Ajbar), mouradb@ksu.edu.sa (M. Boumaaza), humaizi@ksu.edu.sa (K. Alhumaizi)*

Received 31 January 2016; Accepted 4 November 2016

ABSTRACT

A previously validated model for direct contact membrane distillation (DCMD) was used to analyze the performance of a process for desalinating geothermal saline water. The water recovery rate for a single DCMD unit is extremely low. Using several MD units arranged in series and array patterns increases pure water production. Another advantage of the cascade structure is that most of the geothermal energy associated with brackish water is utilized. The number of units that can be used in a series pattern is determined by the temperature difference between the exit brine and inlet permeate streams of an MD unit. The number of stages that can be used in an array pattern is determined by the temperature difference between the exit permeate and brine streams through out the stage. Simulations indicated that 51% water recovery can be achieved when 40 MD units are used in an array pattern. The analysis revealed a16% increase in water recovery when the feed salinity is reduced from 3.7% to 0.2%. In addition, the gained output ratio can reach a value of 9 when the entire exit permeate stream is recycled to the MD unit as a feed stream at the expense of additional waste of heat.

Keywords: Brackish water; Desalination; Membrane distillation; Cascade

1. Introduction

The Kingdom of Saudi Arabia is an arid country with annual renewable water resources of 95 m^3 per capita, substantially below the 1000 m^3 per capita benchmark commonly used to denote water scarcity. Currently, more than half of the potable water needs of Saudi Arabia are satisfied through large, expensive investments in desalination plants equipped with either thermal- or membrane-based reverse osmosis (RO) units. Additional potable water supply is provided by brackish ground water that commonly undergoes cooling, filtration, and finally, purification in RO units. The increasing operating cost of traditional thermal and RO desalination processes are driving search for new and less expensive technologies. Membrane distillation (MD) is a relatively new technology that can be used for water desalination. This study was a part of a research project that analyzes the technical feasibility of using the heat of high-temperature local brackish ground water as a source of energy for the MD process.

MD is a relatively new and rapidly increasing membrane technology that can be used for desalination. Currently, numerous major cities in the kingdom, including its capital,Riyadh, are supplied with a satisfactory proportion of brackish water by desalination using traditional RO units. Water is cooled to approximately 30°C before being introduced to RO units. The heat of the ground water supply can serve as a source of energy for the MD process.

This membrane process has promising applications in the fields of water desalination and/or purification as well as in the treatment of wastewater. The following four configurations are commonly used and investigated [1–2]:

- Direct contact membrane distillation (DCMD),
- Vacuum membrane distillation(VMD),
- Sweeping gas membrane distillation, and
- Air gap membrane distillation (AGMD).

*Corresponding author.

The DCMD configuration is the most common and is used in various applications. Phattaranawik and Jiraratananon [3] reported that the DCMD configuration is easy to set up, has low energy consumption,and produces a high flux of water permeate. In addition, it seems to be particularly suitable for applications involving water separation [3]. The main benefits of the MD process are its simplicity and the small temperature gradients necessary for its operation. Moreover, because the process operates at the liquid–vapor equilibrium, total rejection of macro molecular ions and other nonvolatile components can be achieved [4]. This high rejection rate and the high quality of the purified water observed are almost independent of the feed water salinity. Safavi and Mohammadi [4] analyzed desalination using the VMD of high-salinity water with concentrations ranging from 100 to 300 g/L. In addition, MD systems are simpler than those used in RO plants and are particularly suitable for remote areas. One of the major advantages of the MD process is that the feed water can be heated using any inexpensive energy source (i.e., solar, geothermal, or waste energy using diesel engines or cogeneration plants). The utilization of such low-grade energy sources makes the MD process a promising separation technique. In particular, the use of solar energy to drive MD units has been studied by several authors [5–8]. Compared with solar energy, geothermal energy is not widely used to drive desalination units, even though both are considered low-grade energies. Geothermal sources of high temperature (>150°C) are often used for power generation; however, medium-temperature (100–150°C) and low-temperature (< 100°C) geothermal resources are suitable for direct use, including heating and thermal desalination. Thus, desalination can be achieved using geothermal energy by adopting different methods. Multi-flash distillation (MSF) can be coupled with medium-temperature geothermal energy. An RO unit can also be driven using a geothermal power plant.

Yari [9] conducted an exergy analysis of various types of geothermal processes. Exergy destruction rates were used to quantify the performance of each studied plant. Bourouni et al. [10] conducted an experimental and theoretical study on a geothermal desalination unit in southern Tunisia. The process was based on the humidification and dehumidification of air. Furthermore, Mohamed and El Minshawy [11] studied a geothermal energy-driven humidification–dehumidification process for water desalination. The authors developed both an experimental setup and a computer code for model validation. Mahmoudi et al. [12] examined the potential application of a geothermal energy-driven desalination unit for brackish water and studied its feasibility in arid regions. The authors concluded that desalination of brackish water represents a highly promising field for geothermal energy with the energy output of geothermal energy resources being generally stable. Moreover, Kalogirou [13], in his review on the use of geothermal energy in desalination, reported that the temperature of the ground below certain levels is relatively invariable throughout the seasons. Eltawil et al. [14] concluded that the continuity and predictability of the supply are the main benefits of geothermal energy. Particularly, thermal energy need not be stored. Bouguecha and Dhahbi [15] experimentally studied the effect of feed conditions on the unit performance achieved using a fluidized bed crystallizer and AGMD driven by geothermal energy. AGMD exhibited a low recovery fraction compared with RO, suggesting that the use of MD with geothermal energy should be further studied.

Several studies have proposed and analyzed various arrangements and configurations for improving performance, including the incorporation of a heat recovery device into the MD system [16,17] and the use of a multistage (or multi-effect) concept [17–18]. The multistage concept is well known and commonly used in multiple effect distillation and multistage flash technologies. Applying this concept increases the recovery ratio and reduces the specific energy consumption of the process.

Regarding geothermal energy in Saudi Arabia, several studies have identified thermal springs in the kingdom. Moreover, surface water occurrences were discovered. Al Dayel [19] reported that the temperatures range from 70 to 100°C. Rehman and Shash [20] reported several hot springs with the deep temperature ranging from 50 to 120°C. Hanan and Taleb [21] noted that despite the availability of several geothermal locations in Saudi Arabia, there are currently no serious projects on utilizing geothermal energy for desalination. In addition to these thermal springs, brackish ground water constitutes a critical source of potable water in the kingdom. Riyadh receives about half of its water from five plants designed to treat brackish water. The plants produce potable water with TDS of less than 500 mg/L from more than 30 wells where the salinity is between 1250 and 1750 mg/L. Each well is approximately 1300 m deep with a flow rate of approximately 200 m^3/h and a temperature in the range of 60–70°C [22]. Brackish raw water is treated by pumping it first to cooling towers for lowering the feed temperature to approximately 30°C. The cooled water is softened, clarified, and subsequently conveyed to sand filters before being fed to RO units. Alsuhaibani and Hepbasli [23] evaluated (on the basis of the specific exergy index [24] values) the geothermal resources in the Gizan and Al-Lith regions as low-quality resources, as classified by Lee [25].

Most previous studies have reported a limited water recovery rate for a single MD unit. In the present study, we examine a method for improving the recovery ratio by using multistage MD units. Ground water of characteristics similar to those of brackish water in Riyadh city is used in this study. For such waters, we know that suitable membranes for the MD process are available in the market. Moreover, a cascade configuration can facilitate the optimal utilization of geothermal energy instead of recycling or utilizing geothermal energy as a waste heat. Particularly, we assess the feasibility of using the heat of the high-temperature brackish water from wells as a source of energy to drive the MD process. Different operating conditions and MD unit arrangements for maximizing water recovery are investigated. The analysis is based on a theoretical model developed by Nakoa et al. [26].

2. Model of the DCMD unit

The mechanism of pure water production in a DCMD unit can be explained using the diagram shown in Fig. 1. The unit has a membrane, a thin hydrophobic layer that allows vapor molecules but not liquid water to pass

through its pores. Cold and hot water streams flow on either side of the membrane. The hot water stream is usually saline water or wastewater with a bulk temperature T_f. On the other side, the cold water stream flows with a bulk temperature T_p. The vapor pressure difference generated because of the temperature difference between hot and cold membrane surfaces (T_{mf} and T_{mp}, respectively) forces water on the hot side to vaporize. The vapor diffuses through the membrane pores and condenses on the cold permeate side. The condensate can be collected as highly pure water. One of the main challenges of using an MD unit is that the difference between the temperatures on either side of the membrane ($T_{mf} - T_{mp}$) is lower than its corresponding bulk value ($T_f - T_p$) because of the resistance to heat transfer by convection and conduction. Analogously, the difference in the salinity on either side of the membrane is lower than the difference in the bulk streams of hot and cold water. These phenomena are known as temperature and concentration polarization, respectively. Hence, the driving force for mass transfer decreases, degrading the efficiency of water production.

An MD process involves simultaneous heat and mass transfer operations. Several previous studies have involved modeling heat and mass processes in MD to identify mass and heat fluxes and consequently, water recovery [26–31]. Rather than developing or modifying these MD models, we used the model developed by Nakoa et al. [26] to study the performance of cascaded MD units. This model type uses heat and mass balances on the feed side, cold side, and membrane of the system. It has been widely used in previous studies [27,31]. Appropriate correlations for heat and mass transfer coefficients were used.

The mass flux (J) of vapor transfer through pores is given by

$$J = C_m(P_1 - P_2)\left(\frac{\frac{kg}{m^2}}{s}\right) \tag{1}$$

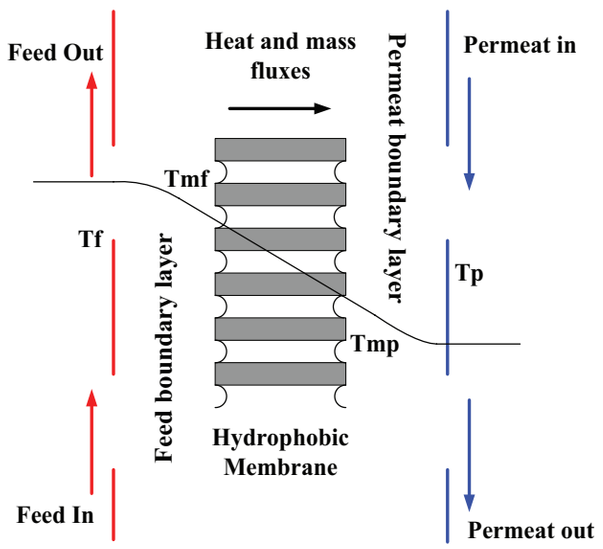

Fig. 1. Boundary layer for a typical DCMD.

In Eq. (1), P_1 and P_2 are the partial pressures of water vapor estimated at the membrane surface temperatures T_{mf} and T_{mp}, respectively. The partial pressure can be calculated using the Antoine equation. C_m is the MD coefficient calculated from three correlations depending on the type of mass transfer regime:

Knudson flow mechanism:

$$C_m^k = \frac{2\varepsilon r}{3\tau\delta}\left(\frac{8M}{\pi RT}\right)^{1/2} \tag{2}$$

Molecular diffusion mechanism:

$$C_m^D = \frac{\varepsilon}{\tau\delta}\frac{PD}{P_a}\frac{M}{RT} \tag{3}$$

Knudsen-molecular diffusion transition mechanism:

$$C_m^C = \left[\frac{3}{2}\frac{\tau\delta}{\varepsilon r}\left(\frac{\pi RT}{8M}\right)^{1/2} + \frac{\tau\delta}{\varepsilon}\frac{P_a}{PD}\frac{RT}{M}\right]^{-1} \tag{4}$$

These different regimes depend on the wall collision theory of water molecules, and each regime dominates at a specific range of values for the mean free path of a water molecule. According to the design parameters used in [26], the Knudsen flow mechanism was found to be suitable and was adopted for the present study. The heat transfer process occurs in three steps:

- Convection from the feed bulk to the vapor–liquid interface at the membrane surface:

$$q_f = h_f(T_f - T_{mf}) \tag{5}$$

- Convection from the vapor–liquid interface at the membrane surface to the permeate side:

$$q_p = h_p(T_{mp} - T_p) \tag{6}$$

where h_f and h_p denote the heat transfer coefficients on the feed and cold stream sides, respectively.

Evaporation and conduction through the micro-porous membrane:

$$q_m = JH_v + h_m(T_{mf} - T_{mp}) \tag{7}$$

where H_v is the water latent heat, where as h_m is the conductive heat transfer coefficient and is equal to k_m/δ, where k_m and δ denote the membrane thermal conductivity and its thickness, respectively.

The total heat flux across the membrane is expressed as follows:

$$q_t = U(T_f - T_p) \tag{8}$$

The overall heat transfer coefficient is given by

$$U = \left[\frac{1}{h_f} + \frac{1}{h_m + \frac{JH_v}{T_{mh} - T_{mp}}} + \frac{1}{h_p}\right]^{-1} \tag{9}$$

Under steady-state operation, the heat transfer in the three individual parts of the system reaches equilibrium:

$$q_f = q_m = q_p \tag{10}$$

Considering the macroscopic scale of the MD unit (Fig. 2), the heat balance around the permeate side is given by [32]:

$$UA(T_f - T_p) = Q_p \rho c_p (T_{p_{out}} - T_{p_{in}}) \tag{11}$$

where Q_p, C_p, and ρ denote the volume flow rate, specific heat at a constant pressure, and density of the permeate, respectively. Similarly, assuming a constant density and heat capacity,the mass and heat balance around the feed side is given by

$$UA(T_f - T_p) = Q_f \rho c_p (T_{b_{out}} - T_{ref}) - Q_b \rho c_p (T_{f_{in}} - T_{ref}) \tag{12}$$

$$Q_f - Q_b = Q_w \tag{13}$$

The definitions of various variables, the numerical values of physical and design parameters, and additional supporting correlations are provided in [26]. Values of some key parameters of the MD unit are listed in Table 1. Eqs. (1)–(9) were solved iteratively until Eq. (10) was satisfied, revealing the mass flux, temperatures on both sides of the membrane, and pure water production. Later, Eqs. (11)–(13) were solved to determine the outlet brine temperature and flow rate ($T_{b_{out}}$ and Q_b, respectively) and the permeate exit temperature ($T_{p_{out}}$) (Fig. 2). The calculated variables were used as feed conditions for the subsequent MD unit. New feed conditions and Eqs. (1)–(9) were solved again for the subsequent MD unit. This procedure was repeated for each MD unit in a given configuration. This procedure was adopted because it is useful for analyzing multiple MD units in series and array patterns. In addition, key threshold values were required to determine the number of feasible units and stages to be used in these patterns; this is described in subsequent sections.

3. Results and discussion

The DCMD model was simulated using the operating conditions described by Nakao et al. [26]. The model was validated for four major variables, namely temperatures and vapor pressures on the hot and cold sides of the membrane (Fig. 3), using the data provided by Nakao et al. [26]. Moreover, other critical variables, such as the heat transfer coefficient and mass transfer coefficient, were in agreement with the values reported by Nakao et al. [26]. The calculated mass flux of the pure water produced is depicted in Fig. 4. The theoretical mass flux in this study matches that reported by Nakao et al. [26] exactly. A mismatch between the model and experimental mass flux values was also observed by Nakao et al. for water salinity of the same magnitude. This discrepancy can be attributed to parametric errors, such as the uncertainty associated with the mass transfer coefficient and/or structural error, whereas lumped parameters were assumed in developing the model. Specifically, the temperature distribution was assumed to be homogenous along both the feed and permeate sides of the membrane. In reality, the temperature on both sides changes along the length of the membrane. However, further model prediction accuracy was not sought in this study. The validated model was used to analyze the DCMD performance in different configurations to maximize the water production, particularly the yield in terms of the ratio of pure water produced to brackish water fed into the system. In all of the following configurations, the water volumetric feed rate is fixed at 2 L/m and the associated temperature is 70°C to resemble the condition at local aquifers. Furthermore, the salt concentra-

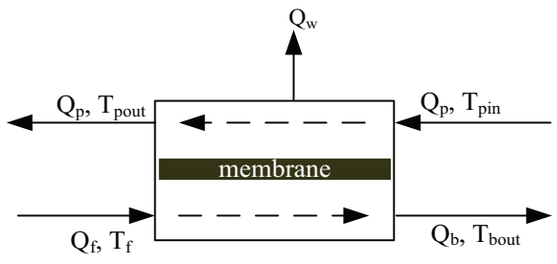

Fig. 2. Typical DCMD unit.

Table 1
Key design parameters of MD unit used

Porosity, e	0.85
Membrane thickness, d	4.5×10^{-5} m
Pore size, d	0.22×10^{-6} m
Hydraulic diameter, d_h	4 mm
Effective surface area, A	0.0572 m²
Hot stream flow rate	2 l/m
Cold permeate flow rate	3 l/m

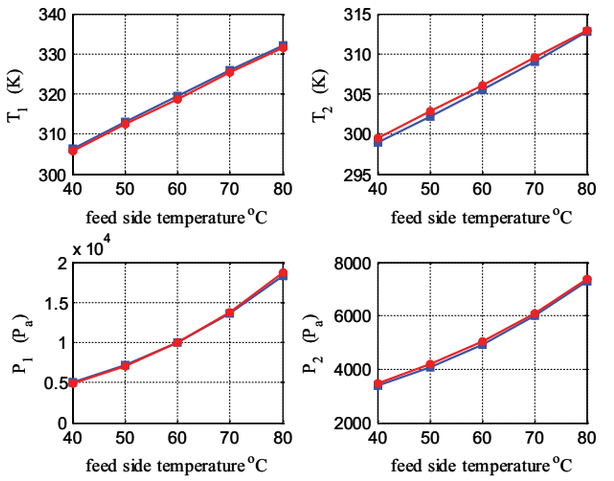

Fig. 3. Validation of the temperature and pressure at the membrane surface, circle: experiment, square: model.

tion is fixed at 3.7% (37,000 ppm), and the inlet temperature of the cold stream is fixed at 20°C.

3.1. Configuration 1: DCMD units in series in one vessel

The pure water production in a single DCMD unit is low (Fig. 4). For a single DCMD unit, the water recovery reaches a maximum value of 7%. In addition, the brine exit temperature is approximately 60°C. Thus, the overall water production can be increased by constructing several DCMD units connected in series (Fig. 5). These units are generally arranged in a single vessel. This configuration enables utilizing most of the geothermal energy inherent in brackish water before the concentrated brine is dumped into the atmosphere. Conceptually, this is analogous to the typical practice adopted in RO desalination plants. RO plants use pressurized feed water. To conserve energy in this process, energy recovery devices are typically used to recover energy from the concentrate stream and transfer it back into the feed flow [33]. The number of DCMD units that can be appended to the system depends on the difference between the brine exit temperature and cold stream inlet temperature. For a series pattern, the following threshold is used:

$$T_{b_{out}} - T_{p_{in}} > 3(K) \tag{14}$$

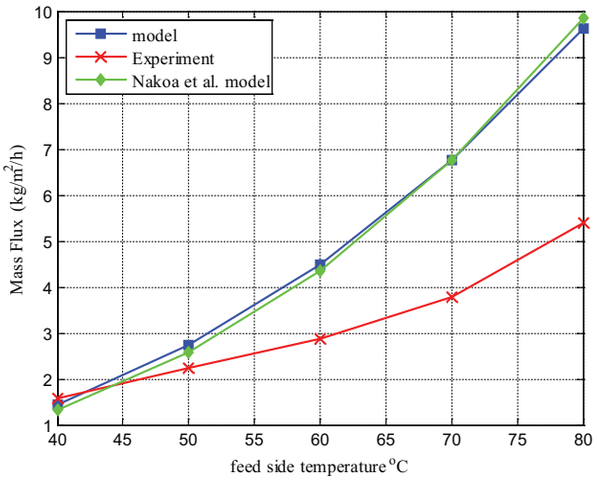

Fig. 4. Experimental and theoretical mass flux at 3.7% feed salinity.

A sufficient difference between $T_{b_{out}}$ and $T_{p_{in}}$ is necessary to activate an additional MD unit in series. This difference enables the development a sufficient driving force for vaporizing the saline water. However, the condition in Eq. (14) cannot be exceeded, because it is physically unstable and leads to infeasible numerical solutions.

The simulation results based on the threshold in Eq. (14) are illustrated in Fig. 6. The results were obtained at a volumetric flow rate of 3 L/m for the cold stream. The maximum achievable number of stages is eight and the individual mass flux as a ratio of the feed decreases with the number of stages because of a decrease in the thermal potential (Fig. 6). However, the accumulated water production increases, with overall production tripling. Fig. 6 illustrates the stage-to-stage variation in the cold and hot stream temperatures (i.e., permeate and brine). The difference between T_b and T_p becomes narrower with the addition of a DCMD unit until the difference becomes small to the extent that adding another unit is infeasible.

An increase in the feed temperature or flow rate improves the performance of a DCMD unit. Because the feed temperature was maintained constant owing to the available resources, we alternatively analyzed the effect of varying the coolant flow rate as a ratio of the hot feed. Fig. 7 shows the effect of the coolant volumetric flow rate on the mass flux of the accumulated pure water. The maximum yield occurs when the two flow rate values are equal (coolant flow rate of approximately 2 L/m), indicating that the optimal performance of a DCMD unit can be achieved when the flow rates of the coolant and feed are equal. The unit performance deteriorates dramatically at low coolant flow rates. Similarly, the maximum allowable number of stages decreases sharply when the flow ratio is slower than 0.75. At small Q_p grades, a large amount of heat is gained by the coolant, leading to a rapid increase in T_p. Therefore, the thermal driving force for subsequent stages substantially decreases. This situation diminishes heat transfer operation, leading to the requirement of fewer stages. In practice, low permeate flow rates should be avoided to prevent overheating of the permeate and infeasible desalination operation. Fig. 7 illustrates the thermal behavior of a DCMD unit at various Q_p values. At low Q_p values, the difference between the feed inlet temperature and permeate outlet temperature remains low and almost constant, indicating that $T_{p_{out}}$ approaches high values in the proximity of T_f. Therefore, using a larger number of stages is impossible. By contrast, the difference between the brine outlet temperature and permeate inlet temperature increases at low Q_p values, indicating that the decreased heat loss overall stages at the feed

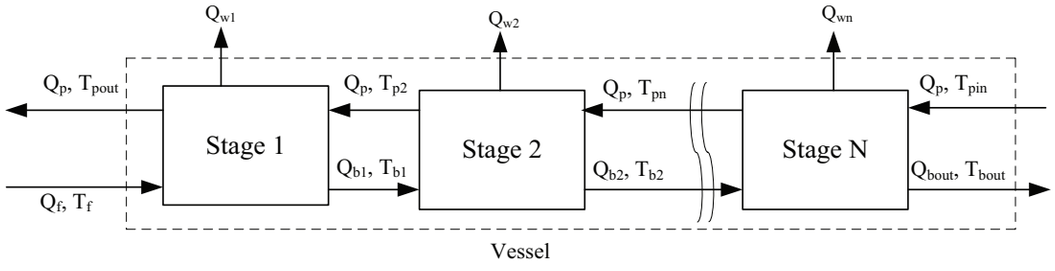

Fig. 5. DCMD units in series using counter current flow scheme.

side lowers the amount of evaporation, resulting in a low yield of pure water. At high Q_p values the outlet permeate temperature deviates from T_f, allowing for room to include additional DCMD stages. However, this is limited because of the decreasing thermal driving force at the other end ($T_{b_{out}} - T_{p_{in}}$). The decreasing value of $T_{b_{out}} - T_{p_{in}}$ indicates that a large amount of heat is transferred from the feed side to the permeate side overall stages, indicating evaporation of a higher amount of water and confirming a higher water yield at considerable Q_p values.

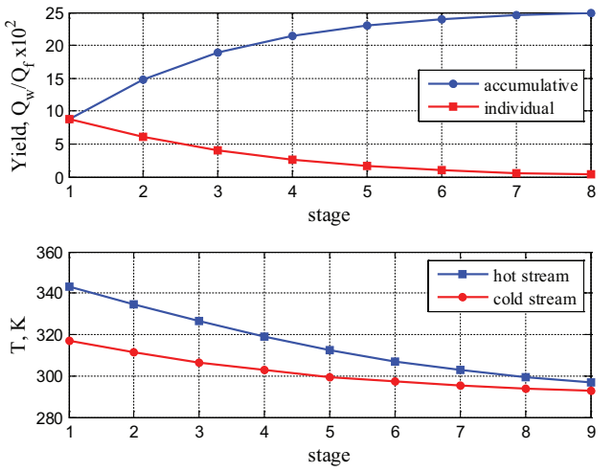

Fig. 6. DCMD performance using configuration in Fig. 5 at Q_p = 3 L/m.

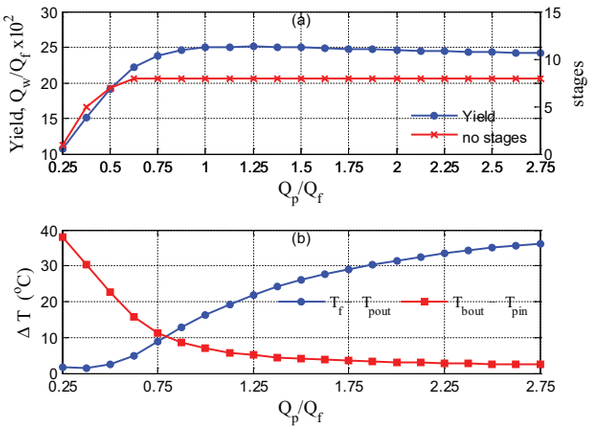

Fig. 7. Variation of pure water yield with coolant flow rate.

3.2. Configuration 2: DCMD units in series with recycling

Fig. 6 shows that the exit temperature of the cold stream approaches a high value, indicating that some geothermal energy is used to produce the pure water through evaporation and the rest is transferred to the cold stream. The permeate stream is commonly recycled to the feed stream to use the potential energy of the recycle stream. Configuration 2 is shown in Fig. 8. To maintain the same operating conditions, the recycle stream is heated to a temperature identical to that of the feed. The pure water production rate remains the same; however, the yield increases, because the makeup feed is reduced by an amount equal to that of the recycled feed. The drawback of this configuration is the requirement of additional energy, which can be fulfilled using waste heat. An energy analysis of configuration 2 is provided in Table 4 and is discussed later in comparison with the other configurations.

3.3. Configuration 3: DCMD units in an array pattern

Another approach for consuming the energy associated with the permeate outlet flow is to connect another DCMD vessel in series (Fig. 9). In this configuration, the hot permeate exiting the first vessel enters the second vessel as a feed for the second cycle, and the cooled brine outlet of the first vessel enters the second vessel as a cold stream (permeate). A bank of DCMD units consists of several parallel vessels, with each vessel consisting of several DCMD units.

For the array pattern, the following threshold is used:

$$T_{p_{out}} - T_{b_{out}} > 3(K) \tag{15}$$

The difference between $T_{p_{out}}$ and $T_{b_{out}}$ must be sufficiently large to activate the next cycle of a chain of MD units connected in series (Fig. 9). The number of DCMD units present in each vessel is limited by the difference between the temperature of the exit brine and that of the inlet permeate of the final MD unit in the same vessel. Conversely, the number of parallel vessels is limited by the difference between the temperature of the exit permeate of the first MD unit and that of the exit brine of the final MD unit in the same vessel. Each set of vessels in this configuration is called a cycle. A common and single feed with a unique value is used in all configurations for a

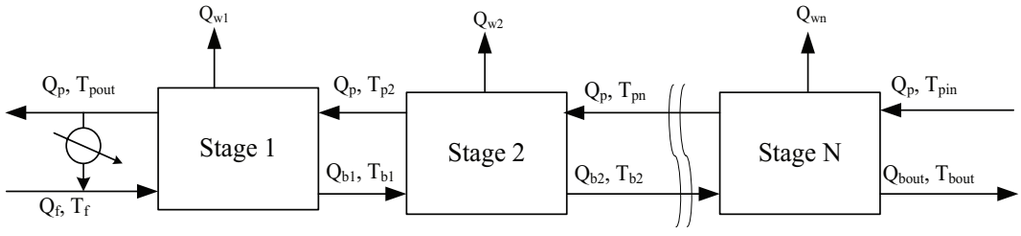

Fig. 8. Configuration 2, consecutive stages with a recycle.

fair comparison. The maximum feed flow that a vessel or bank can manage is limited by the diameter of the associated MD unit. For higher feed flow rates, multiple parallel sets of banks or vessels with multiple independent feeds can be used. Fig. 10 depicts the simulation results for this configuration obtained using a Q_p value of 2 L/m and the thresholds given by Eqs.(14) and (15).

Under the given operating conditions, the simulations indicated that a maximum of three cycles can be managed, with each cycle having an obviously decreasing number of maximum allowable MD units. The first cycle has the highest water production. The yield in each cycle is based on its own fresh feed. The overall yield shown in the same diagram is based on the amount of original feed (brackish water fed into the first cycle).The accumulated water production increases with a repeated set of cycles. Up to 35% of water recovery is achieved, as Fig. 10 illustrates. The thermal behavior of the cascade system is also depicted in Fig. 10. The discrepancy between the permeate outlet temperature and brine outlet temperature is the driving force for a subsequent cycle. The driving force increases after the first cycle of water production, but decreases subsequently with the addition of MD units until it converges to a minor value insufficient to power any additional cycle. At this stage, most of the potential thermal energy is utilized.

We also investigated the sensitivity of configuration 3 to variation in the flow rate of the cold stream. The simulations were repeated at Q_p =1 L/m and 3 L/m. The outcome of the analysis is shown in Fig. 11a. Operating at Q_p =2 L/m, which is equal to the brackish water feed rate, yields the optimal water recovery ratio. Fig. 11a shows the optimal performance of configuration 1 for comparison purposes. The superiority of the parallel arrangement over a simple series arrangement was confirmed even at the lowest permeate feed rate. However, the total number of DCMD units used in the configurations varies. Typically, the capital investment and operational cost are directly proportional to the number of MD elements involved. Therefore, the performance of the configurations per capita was compared by dividing the water yield by the total number of MD units. The comparison is illustrated in Fig. 11b. The situation is reversed when the array pattern performance at the lowest permeate feed has the lowest cost of production. Moreover, configuration 2 out performs the other configurations according to the production cost because it requires the lowest number of MD units.

In configuration 3 (Fig. 10), the brine exiting the first cycle enters the following cycle as a cold permeate stream. Although the brine outlet is cooled, it does not reach the temperature of the original cold stream fed into the first cycle. Thus, the efficiency of the subsequent cycles degrades rapidly. Using afresh cold stream at each cycle is necessary (Fig. 12). Repeating the simulation with Q_p = 2 L/m and T_p = 20°C for each cycle improved the performance (Fig. 13). The global recovery approaches 51%, which is equivalent to a 45% increase compared with the value achieved using a common feed for the cold stream. However, this improvement occurs at the expense of requiring a higher number of MD units (40 MD units) than for setting up a common feed. Moreover, the modified setup consumes a

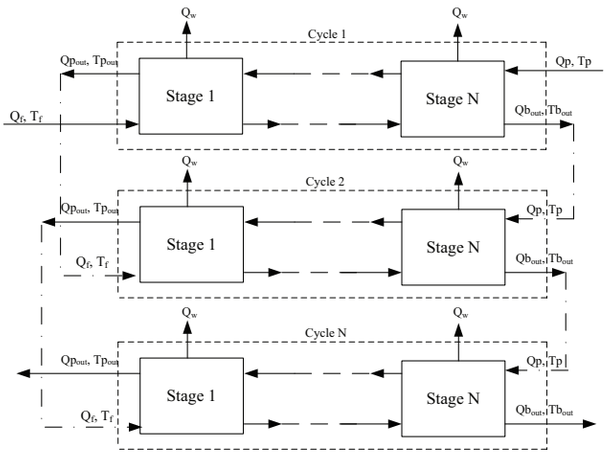

Fig. 9. Configuration 3; Cascade of parallel vessels.

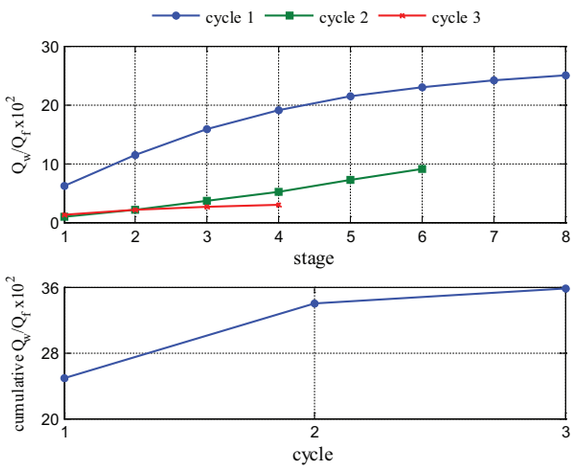

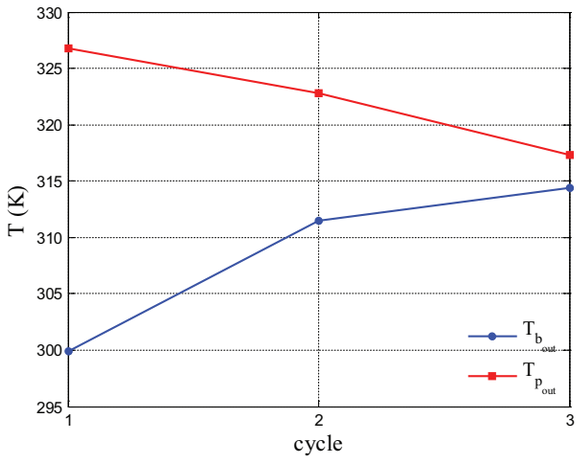

Fig. 10. Configuration 3 behavior at Q_p = 2 L/m.

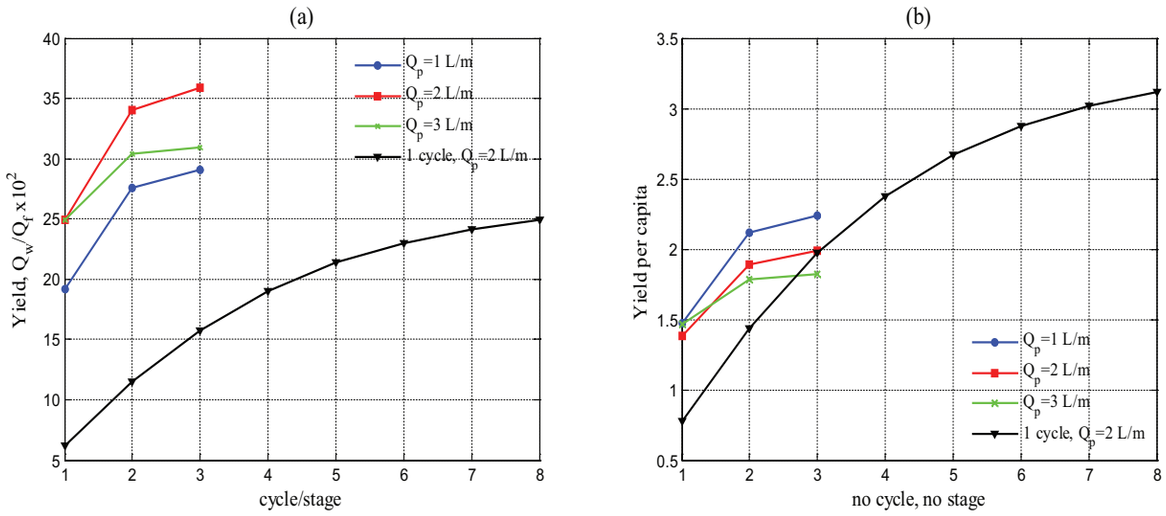

Fig. 11. Sensitivity of water yield of configuration 3 with respect to permeate feed rate; (a) Raw yield, (b) Yield per capita.

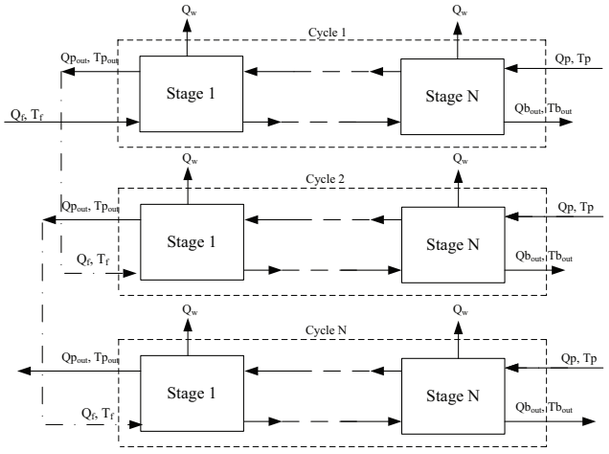

Fig. 12. Configuration 3; Cascade of parallel vessels with independent coolant feed.

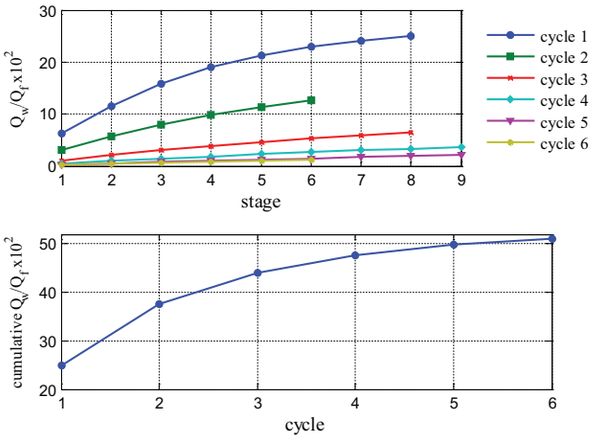

Fig. 13. Configuration 3 behavior with independent coolant feed for each cycle with Q_p = 2 L/m.

higher amount of water as a coolant stream. In this configuration, a fixed cold permeate stream is used in each cycle, enabling the threshold given by Eq. (15) to be fulfilled by increasing the number of cycles. Increasing the number of cycles is a crucial factor for increased water production. Table 2 summarizes the analysis results regarding the recovery ratio and total required number of MD units for all configurations.

The aforementioned tests were conducted at a salinity of 3.7%, which is suitable for seawater. The salinity of brackish water from geothermal sources is substantially lower. Thus, to assess the effect of water salinity on the performance of MD units, the simulations were repeated using three salt concentrations. The results are listed in Table 3. The process performance for all configurations improves with a decrease in the salinity, thus coinciding with the results reported by Nakoa et al. [26]. This finding confirms the suitability of MD technology for desalinating geothermal water sources. For further assessing and comparing the analyzed configurations, two key performance indicators (KPIs) were examined (Table 4). The first KPI was the concentration factor (C_r), defined as the ratio of the salt concentration in the final exiting brine to the initial salt concentration in the initial feed. Calculating the salt concentration of the rejected brine is crucial because the concentrate side of the membranes is the area where fouling and scaling occur. Thus, the maximum salt content in the brine determined by the solubility of the salt should be limited. Gebel and Yuce [34] considered 60,000 ppm (6%) the maximum value for the brine concentration to avoid scaling. Therefore, for a feed salinity of 3.7%, the C_r is 1.62. This value is extremely close to the highest C_r value of 1.64 (Table 4). Therefore, the salinity of the brine at the outlet of the MD unit is somehow higher than that of the feed. The risk of fouling and scaling remains moderate at these C_r values. Table 4 indicates that the C_r is slightly higher for MD units in the array pattern.

Table 2
Technical comparison of the 3 configurations

	Total number of units used	% recovery
Conf. #1 and 2	8	25
Conf. #3 with interchanging cold feed	18	35
Conf. #3 with independent cold feed	40	51

Table 3
Effect of salinity of water recovery at Q_p = 3 l/m

Salinity	3.7%	1.5%	0.2%
Conf. #1	24.9	26.4	27.5
Conf. #3 with interchanging cold feed	30.1	32.3	34.4
Conf. #3 with independent cold feed	42.9	47.5	50.0

Table 4
Effect of salinity of water recovery at, 3.7% salinity

Flow rate	Q_p = 2 l/m		Q_p = 3 l/m	
KPI	C_r	GOR	C_r	GOR
Conf. #1	1.58	2.58	1.606	2.5
Conf. #2 with 50% recycle	1.58	4.05	1.606	3.42
Conf. #2 with 100% recycle	1.58	8.76	1.606	4.98
Conf. #3 with interchanging cold feed	1.64	3.57	1.62	3.15
Conf. #3 with independent cold feed	–	5.34	–	4.53

The C_r should be higher because of the larger number of units used. The circulating brine does not pass through all cycles as a flashing stream. Nevertheless, it is sometimes used as a cold permeate, specifically in the even-numbered cycles. This KPI is not reported for configuration 3 with the independent cold feed, because the brine stream is not circulated through all cycles.

The other KPI analyzed was the gained output ratio (GOR), defined as

$$GOR = \frac{m_{wtotal} A H_v}{H_{in}} \tag{16}$$

where H_{in} is the total energy supplied to the system and m_{wtotal} is the accumulated pure water production rate. H_{in} can be expressed in terms of the initial feed mass flow rate m_f and its temperature T_f as

$$H_{in} = m_f C_{pf} (T_f - T_{ref}) \tag{17}$$

The thermal efficiency is the ratio of the heat energy consumption for water vaporization to the total energy supplied to the system through the initial fresh feed. Usually, GOR is defined as the ratio of the fresh water produced to the mass of saturated steam delivered to the system. In the absence of direct use of steam as the source of energy, the thermal efficiency is used here as alternative definition of GOR [35]. H_{in} is the sensible heat associated with the hot feed in configurations 1 and 3. For configuration 2, H_{in} is simply the amount of heat supplied to the heat exchanger required to heat the recycle stream (Fig. 8) to achieve the desired temperature. The higher the value of this KPI is, the more enhanced the process performance. The GOR for configuration 3 is higher than that for configuration 1 because of the larger number of units involved. Configuration 2 with 100% recycling exhibited the optimal thermal performance, because H_{in} is the smallest in this configuration. The amount of heat required is small because the difference between the temperature of the hot feed, T_f, and the temperature of the permeate outlet, T_{pout}, is small (Stage 1 in Fig. 6). This finding has commonly been reported in the literature because waste heat is sufficient to heat the recycle stream. Nevertheless, geothermal energy is not properly utilized in this case, because only the cold stream is fed into the MD unit when 100% recycling is used. Thus, geothermal energy should be used as a heating medium for the heat exchanger in configuration 2. However, a fraction of geothermal energy is lost because of the limited efficiency of the heat exchanger. Except in configuration 1, the thermal performance is superior at the lower cold permeate flow rate. At the higher cooler feed rate(3 L/min), the amount of heat absorbed leads to a lower T_{Pout} value. Therefore, the threshold defined by Eq. (15) does not apply, resulting in a lower number of cycles. Moreover, a large amount of heat energy is acquired from the hot stream, leading to a lower $T_{b_{out}}$ and causing the condition imposed by Eq. (14) to diminish in each subsequent cycle. Consequently, a lower number of MD units is used in each sub-cycle. Overall, the amount of energy consumed for evaporation is reduced, leading to a smaller GOR value. The estimated values for GOR are typically within the range reported in the literature. Summers et al. [36] reported GOR values ranging from 0.17 to greater than 4. AGOR value greater than 4 corresponds to an MD unit with eight stages in series. In addition, Saffarini et al. [37] reported GOR values for various existing solar-powered MD systems ranging from 0.3 to 6.

The recovery ratio values reported in previous studies, such as Saffarini et al. [37], are very low, because the systems used were typically of a single-stage type and simple (not compact). One of the benefits of cascading and multistage systems is an increase in the recovery ratio. The recovery ratio values obtained in the present study reach 50%. The overall recovery ratios for two major conventional technologies, namely MSF and SWRO, can be 10%–20% and 20%–50%, respectively [38].

It should be noted though, the multiplicity of units and vessels may require additional pumping energy to compensate for the pressure drop in order to keep each subsequent unit operating at atmospheric pressure. In this paper, it is assumed that an inter-stage pump is in service to maintain water circulation at required pressure. The unit pressure drop is estimated to be around 0.2 bar [39,40] for the given flow rate used here. Therefore, the energy associated with pumping is relatively small compared to the energy

associated with the hot water feed. Note that using a pressurized brackish water feed of 4 bar (assuming the maximum allowable LEP is around 4 bar [41]) and assuming the pressure drop in a single membrane is 0.2 bar [39,40], a maximum 20 stages in series can be handled without the need of inter-stage pumps. This makes our results practical because,in our findings, the maximum number of stages in series using the same water feed is found to be 9.

4. Conclusions

A theoretical model for DCMD units developed by Nakoa et al. [26] was applied and validated using data published in the literature. The desalination operation was conducted using brackish water with a geothermal temperature of 70°C, which mimics conditions at local aquifers in Saudi Arabia. The model was used to analyze the performance of a process for maximizing the recovery by optimally utilizing the energy resources associated with the feed water. Setting several MD units in series increases the overall water recovery to 25%. The overall water recovery is limited by the total number of MD units that can be constructed, which is controlled by the temperature difference between the inlet permeate and outlet brine and is influenced by the flow rate of the cold permeate. A thermal analysis of the exit brine and permeate temperatures demonstrated the potential for further utilization of the inherent geothermal energy by arranging the DCMD units in an array pattern. The array pattern shows an up to 35% increase in the yield,but requires higher investment because a larger number of units is involved. The maximum allowable number of cycles (rows in the array pattern) is controlled by the temperature difference between the exit brine and exit desalinate. The yield of this configuration can be increased to 51% when fresh cold permeate is fed into each cycle. However, the total number of MD units involved and cold water consumption also increases. The flow rate of the cold stream substantially affects all configurations. An optimal performance was observed at equal flow rates for the hot and cold feeds.

Acknowledgment

This study was funded by the National Plan for Science, Technology and Innovation (MAARIFAH), King Abdulaziz City for Science and Technology, Kingdom of Saudi Arabia, (12-WAT2616-02).

Symbols

A	—	Surface area, m²
C_m^k	—	Knudsen mass flux coefficient, kg/m²·s·Pa
C_m^d	—	Moléculaire diffusion mass flux coefficient, kg/m²·s·Pa
C_m^C	—	transition mass flux coefficient, kg/m²·s·Pa
c_p	—	Heat capacity, j/kg K
d_h, d	—	Hydraulic and pore diameter, m
H_v	—	Latent heat of vaporization, J/kg
h_f, h_p, h_m	—	Feed, permeate and membrane heat transfer coefficient, W/m² K
J	—	Mass flux, kg/m² h
k_m	—	Membrane conductivity, W/m K
M	—	Molecular weight of water, gm/mole
P_1, P_2	—	Vapor pressure at feed and permeate membrane surface, Pa
PD	—	Membrane pressure multiplied by diffusivity, Pa·m²/s
P_a	—	Entrapped air pressure, Pa
q_f, q_p	—	Heat transfer rate at feed and permeate sections, W/m²
Q_p, Q_f, Q_w, Q_b	—	Permeate, feed, pure water, and brine flow rate, l/m
Q_t	—	Overall heat flux, W/m²
Q	—	Heat flow to the system, J/s
R	—	Ideal gas constant, J/mole K
T_p, T_f	—	Feed and permeate bulk temperature, K
T_{mf}, T_{mp}	—	Feed and permeate membrane temperature, K
T_{ref}	—	Reference temperature, K
U	—	Overall heat transfer coefficient, W/m²·K
ε	—	Porosity
τ	—	Membrane tortuosity
δ	—	Membrane thickness, mm
ρ	—	Density kg/m³

References

[1] J. Orfi, N. Loussif, Modeling of a membrane distillation unit for desalination, Book Chapter, in Desalination: Methods Costs and Technology. I.A. Urboniene, ed., Nova Science Publishers, NY, 2010, pp. 143–174.
[2] M.S. El-Bourawi, Z. Ding, R. Ma, M.A. Khayat, Framework for better understanding membrane distillation separation process. J. Membr. Sci., 285 (2006) 4–29.
[3] J. Phattaranawik, R. Jiraratananon, Direct contact membrane distillation: effect of mass transfer on heat transfer, J. Membr. Sci., 188 (2001) 137–143.
[4] M. Safavi, T. Mohammadi, High-salinity water desalination using VMD, Chem. Eng. J., 149 (2009) 191–195.
[5] F. Macedonio, E. Drioli, Pressure-driven membrane operations and membrane distillation technology integration for water purification, Desalination, 223 (2008) 396–409.
[6] H.E.S. Fath, SM. Elsherbiny, A.A. Hassan, M. Rommel, M. Wieghaus, J. Koschikowski, M. Vatansever, PV and thermally driven small-scale, stand-alone solar desalination systems with very low maintenance needs, Desalination, 225 (2008) 58–69.
[7] J. Koschikowski, M. Wieghaus, M. Rommel, V.S. Ortin, B.J. Suarez, R.B. Rodríguez, Experimental investigations on solar driven stand-alone membrane distillation systems for remote areas, Desalination, 248 (2009) 125–131.
[8] T.-C. Chen, C.-D. Ho, Immediate assisted solar direct contact membrane distillation in saline water desalination, J. Membr. Sci., 358 (2010) 122–130.
[9] M. Yari, Exergetic analysis of various types of geothermal power plants. Renew. Energy, 35 (2010) 112–121.
[10] K. Bourouni, J.C. Deronzier, L. Tadrist, Experimentation and modelling of an innovative geothermal desalination unit, Desalination, 125 (1999) 147–153.
[11] A. Mohamed, N. El Minshawy, Humidification–dehumidification desalination system driven by geothermal energy, Desalination, 249 (2009) 602–608.
[12] H. Mahmoudi, N. Spahis, M. Goosen, S. Sablani, S. Abdul-wahab, N. Ghaffour, N. Drouiche, Assessment of wind energy to power solar brackish water greenhouse desalination units: A case study from Algeria, Renew. Sustain. Energy Rev., 13 (2009) 2149–2155.

[13] S. Kalogirou, Seawater desalination using renewable energy sources, Progr. Energy Combust. Sci., 31 (2005) 242–281.
[14] M.A. Eltawil, Z. Zhengming, L. Yuan, A review of renewable energy technologies integrated with desalination systems, Renew. Sustain. Energy Rev., 13 (2009) 2245–2262.
[15] S. Bouguecha, M. Dhahbi, Fluidised bed crystalliser and air gap membrane distillation as a solution to geothermal water desalination, Desalination, 152 (2003) 237–244.
[16] G. Guan, X. Yang, R. Wang, A.G. Fane, Evaluation of heat utilization in membrane distillation desalination system integrated with heat recovery, in press, Desalination, 2015.
[17] E. Drioli, A. Ali, F. Macedonio, Membrane distillation: Recent developments and perspectives, Desalination, 356 (2015) 56–84.
[18] H. Geng, J. Wang, C. Zhang, P. Li, H. Chang, High water recovery of RO brine using multi-stage air gap membrane distillation, Desalination, 355 (2015) 178–185.
[19] M. Al Dayel, Geothermal resources in Saudi Arabia, Geothermics, 17 (1988) 465–476.
[20] S. Rehman, A. Shash, Geothermal Resources of Saudi Arabia – Country Update Report, Proceedings World Geothermal Congress 2005, Antalya, Turkey, 24–29 April 2005.
[21] H.M. Hanan, M. Taleb, Barriers hindering the utilisation of geothermal resources in Saudi Arabia, International Conference and Exhibition on Green Energy & Sustainability for Arid Regions & Mediterranean Countries, Le Royal Hotel Amman, Jordan, November, 10–12, 2009.
[22] R.I.S. Al Mudaiheem, S.O.A. Al Yousef, T. Sharif, A.K.M. Amirul Islam, Performance evaluation of ten years operation experience of brackish water RO desalination in Manfouha plants, Riyadh, Desalination, 120 (1998) 115–120.
[23] Z. Alsuhaibani, A. Hepbasli, Future directions of geothermal energy in Saudi Arabia, energy sources, Part A: Recovery, utilization, and environmental effects, 2010 (in Press).
[24] A. Hepbasli, A review on energetic, exergetic and exergo economic aspects of geothermal district heating systems (GDHSs), Energy Convers. Manage., 51 (2010) 2041–2061.
[25] K.C. Lee, Classification of geothermal resources by exergy. Geothermics, 30 (2001) 431–442.
[26] K. Nakoa, A. Date, A. Akbarzadeh, A research on water desalination using membrane distillation, Desal. Water Treat., 56(10) (2015) 2618–2630.
[27] M. Khayet, Membranes and theoretical modeling of membrane distillation: a review, Adv. Colloid Interf. Sci., 164 (2011) 56–88.
[28] A. Al-Anezi, A. Sharif, M. Sanduk, A. Khan, Experimental investigation of heat and mass transfer in tubular membrane distillation module for desalination, ISRN Chemical Engineering, doi:10.5402/2012/738731.
[29] D. Lawal, A. Khalifa, Flux prediction in direct contact membrane distillation, Int. J. Mater. Mech. Manufact., 2(4) (2014) 302–308.
[30] E. Close, E. Sorensen, Modeling Direct Contact Membrane Distillation for Desalination, 20th Symposium on Computer Aided Process Engineering, S. Pierucci and G. Buzzi Ferraris, eds., 2010, Elsevier.
[31] A. Alkhudiri, N. Darwish, N. Hilal, Membrane distillation: a comprehensive review, Desalination, 287 (2012) 2–18.
[32] J. Zhang, Theoretical and experimental investigation of membrane distillation, PhD thesis, Victoria University, Australia, 2011.
[33] S. Schreck, Integrated Wind energy Desalination System, National Renewable energy laboratory, subcontract report, Niskayuna, New York October 2006.
[34] J. Gebel, S. Yuce, An Engineer's Guide to Desalination, VGB PowerTech, Germany, 2008, p. 506.
[35] A.K. Fard, Y.M. Manawi, T. Rhadfi, K.A. Mahmoud, M. Khraisheh, F. Benyahia, Synoptic analysis of direct contact membrane distillation performance in Qatar: A case study, Desalination, 360 (2015) 97–107.
[36] E. Summers, J.H. Lienhard V, Experimental study of thermal performance in air gap membrane distillation systems, including the direct solar heating of membranes, Desalination, 330 (2013) 100–111.
[37] R.B. Saffarini, E.K. Summers, H.A. Arafat, J.H. Lienhard V, Technical evaluation of stand-alone solar powered membrane distillation systems, Desalination, 286 (2012) 332–341.
[38] T. Bleninger, G.H. Jirka, Environmental planning, prediction and management of brine discharges from desalination plants, Final Report, Middle East Desalination Research Center, MEDRC Project: 07-AS-003, Muscat, Oman, Dec. 2010, p. 237.
[39] D. Winter, J. Koschikowski, M. Wieghaus, Desalination using membrane distillation: Experimental studies on full scale spiral wound modules, J. Membr. Sci., 375 (2011) 104–112.
[40] K.K. Sirkar, L. Song, Pilot-Scale Studies for Direct Contact Membrane Distillation-Based Desalination Process, U.S. Department of the Interior, Bureau of Reclamation, DWPR Report No. 134, 2009.
[41] Y. Tzahi, Cath, V.D. Adams, A.E. Childress, Experimental study of desalination using direct contact membrane distillation: a new approach to flux enhancement, J. Membr. Sci., 228 (2004) 5–16.